Journal of the European Ceramic Society **18** (1998) 1565–1570

PII: S0955-2219(98)00078-8
0955-2219/98/$—see front matter

Grain Boundary Segregation in High-purity, Yttria-stabilized Tetragonal Zirconia Polycrystals (Y-TZP)

Susanne Stemmer, Jozef Vleugels and Omer Van Der Biest*

Department of Metallurgy and Materials Engineering, Katholieke Universiteit Leuven, de Croylaan 2, B-3001 Leuven, Belgium

(Received 24 December 1997; accepted 16 February 1998)

Abstract

In this paper, we use high-resolution transmission electron microscopy and electron energy-loss spectroscopy to study the microstructure of grain boundaries and the segregation of yttrium, respectively, in yttria-stabilized tetragonal polycrystalline zirconia, sintered from different high-purity powders. No amorphous films were observed at the grain boundaries, and only the sample containing the highest amount of silicon impurity showed presence of an amorphous silicate phase in all triple grain junctions. A strong yttrium segregation to the grain boundaries is observed in all samples, despite different grain sizes and impurity levels. © *1998 Elsevier Science Limited. All rights reserved*

1 Introduction

Grain boundary segregation of impurities and stabilizing dopants in polycrystalline ZrO_2 (zirconia) is an important issue for many applications of these materials. For example, impurity segregation has been shown to lower the specific grain boundary conductivity in stabilized zirconia polycrystals used as solid electrolytes.[1] Grain growth in zirconia is known to be dependent on the impurity and dopant segregation to the grain boundaries,[2,3] and different mechanisms have been proposed.[2–5] Tailoring of the grain size is very important for structural applications of zirconia ceramics, since the high toughness of zirconia, which is due to the transformation toughening mechanism, depends on the grain size and yttria concentration dependent maintaining of the transformable tetragonal modification after sintering.[6]

Previous studies in literature have investigated the segregation of dopants and impurities in polycrystalline zirconia. However, most of these studies were performed on materials containing a significant amount of impurities, especially SiO_2, which often forms a grain boundary wetting amorphous film. In most cases these studies used surface analytical methods, like X-ray photoelectron spectroscopy (XPS) or Auger electron spectroscopy (AES), and studied the segregation on intergranular fracture surfaces.[2–4,7] Some authors[8,9] claim that the yttria enrichment of the grain boundary is correlated with the often observed wetting of the grain boundary by a silicate phase. In high-purity, stabilized zirconia, grain boundaries were found to be free of amorphous phases.[1,10,11]

In a recent study Aoki *et al.*[1] investigated the silicon impurity segregation with a very high-spatial resolution by energy-dispersive X-ray spectroscopy (EDS) in high-purity fully calcia-stabilized zirconia that contained no continuous amorphous grain boundary films.

They showed a grain-size dependent co-segregation of calcium and silicon to the grain boundaries. In the grain boundaries of the material with the finest grain size no silicon was detected.

In the present study, we were interested in the influence of residual impurities on the microstructure of high-purity yttria-stabilized tetragonal zirconia polycrystals (Y-TZP) and in the grain boundary segregation of the dopant yttrium. For analyzing the composition of the grain boundaries we chose electron energy-loss spectroscopy (EELS) in a transmission electron microscope (TEM), in order to study the chemistry of internal interfaces,

*To whom correspondence should be addressed. Fax: 0032 16 321992; e-mail: omer.vanderbiest@mtm.kuleuven.ac.be

such as grain boundaries and triple pockets, with a very high spatial resolution.

2 Experimental

Y-TZP were prepared from three different commercially available powders, doped with about 3 mol% yttria. These powders contained only a very low amount of impurities, though slight differences exist between the three powders. The compositions of the three different powders, according to the respective manufacturers, are given in Table 1. The first two powders (Tosoh and Daiichi) are produced by co-precipitation of ZrO_2 and Y_2O_3 from a solution. The other powder (Tioxide), is formed by plasma decomposition of $ZrCl_4$ and subsequent Y_2O_3 coating.[12] Please note that the powders 2 and 3 in Table 1 quote an even lower SiO_2 and Al_2O_3 impurity concentration than powder 1 (Daiichi).

Y-TZP samples were obtained by hot-pressing in BN coated graphite dies under vacuum (applying a mechanical load of 28 MPa) for 1 h at 1450°C, using a heating rate of 50 K/min and a cooling rate of 10 K/min. The ceramics produced from the three different powders showed different mechanical properties, the fracture toughness values K_{Ic} (as obtained by the Vickers H_{V5} indentation technique, and calculated according to[13] were determined to be 3·6 MPa $m^{1/2}$ (ceramic from powder 1), 2·5 MPa $m^{1/2}$ (powder 2) and 8·9 MPa $m^{1/2}$ (powder 3), respectively. These results confirm observations of other authors that found improved mechanical properties of Y-TZP sintered from plasma-coated powders.[14] Average grain sizes in the Y-TZP were determined from scanning electron micrographs of polished and thermally etched surfaces, and found to be 0·36, 0·27 and 0·17 μm for the materials sintered from powders 1, 2 and 3 respectively.[15]

Transmission electron microscopy (TEM) samples were prepared by standard TEM preparation methods, including ion-milling at 5 kV under an angle of 12° until perforation. Coating of the samples with a thin layer of carbon was necessary to prevent charging under the electron beam. TEM observations were performed in an instrument equipped with a field-emission gun operating at 200 kV (Philips CM200 FEG) and a point-to-point resolution of 2·3Å. High-resolution (HRTEM) TEM micrographs were recorded using a slow scan CCD camera. For HRTEM imaging of grain boundaries, only those between grains oriented close to a low-indexed zone axis, and with the grain boundary plane oriented parallel to the electron beam are suitable. EEL spectra were recorded employing a post-column imaging filter (Gatan GIF200). All spectra presented in this paper were recorded using a nominal probe size of 1·5 nm. To analyze the segregation of impurities and dopants to the grain boundaries, one EEL spectrum containing the respective ionization edges (Si K-edge, Y and Zr L-edges) was recorded directly on the grain boundary and a second spectrum next to it, at a distance of about 5 nm from the grain boundary. Preliminary results showed that the segregation was confined to an area of less than 5 nm around the grain boundary plane, in accordance with results of Aoki *et al.*[1] After appropriate background subtraction, edge counts were extracted by integration over the respective $YL_{2,3}$ and Zr $L_{2,3}$-edges over an energy window, and Y/Zr count ratios were obtained from spectra recorded on the grain boundaries and in the adjacent grains.

3 Results

Figure 1(a)–(c) shows low-magnification TEM micrographs of the Y-TZP samples sintered from the three different powders. Differences in grain size are also obvious from these TEM micrographs, with the samples sintered from powder 3 exhibiting the smallest grain size. Investigations of the overall microstructure were performed, and are only summarized here. Materials sintered from powder 3 contained, besides the major tetragonal phase, some amount of large cubic grains, and also grains in the monoclinic modification. These grains were believed to have transformed during TEM sample preparation, since the presence of the monoclinic phase was not detected in a prior X-ray diffraction analysis within the detection limit of this method (about 5 vol%). The presence of monoclinic grains can therefore serve as an indication for the higher transformability of this material, leading to higher fracture toughness values measured in those specimens. In the micrographs of the three specimens triple and multiple grain

Table 1.

Powder (manufacturer)	*Y_2O_3 (wt%)*	*Al_2O_3 (wt%)*	*SiO_2 (wt%)*	*HfO_2 (wt%)*	*Fe_2O_3 (wt%)*	*Na_2O (wt%)*
Powder 1 (Daiichi HSY3)	5·4	0·25	0·11	≈2	0·0003	0·03
Powder 2 (Tosoh TZ-3Y)	5·2	<0·005	0·006	≈2	0·003	0·021
Powder 3 (Tioxide YZ5N	5·2	0·09	<0·01	1·6	<0·01	<0·01

pockets are sometimes visible and are indicated in Fig. 1. Figure 2 shows a HRTEM micrograph of the amorphous phase in a triple pocket in ceramic sintered from powder 1. The ceramics sintered from powder 1 showed the presence of an amorphous phase in all triple grain junctions that were examined. The diameter of those pockets was found to be between 2 and 10 nm. In the other two samples, amorphous phase was present mainly in large multiple grain pockets, and only occasionally in triple grain junctions. Figure 3 shows a typical HRTEM micrograph of a grain boundary in a sample sintered from powder 1. No continuous amorphous film can be observed, though some regions show a slightly 'disordered' structure. Also in the other two ceramics, no amorphous intergranular films were observed.

In the following, we present the results of the EELS analysis of triple pockets and grain boundaries in the three different polycrystals. Figure 4(a)

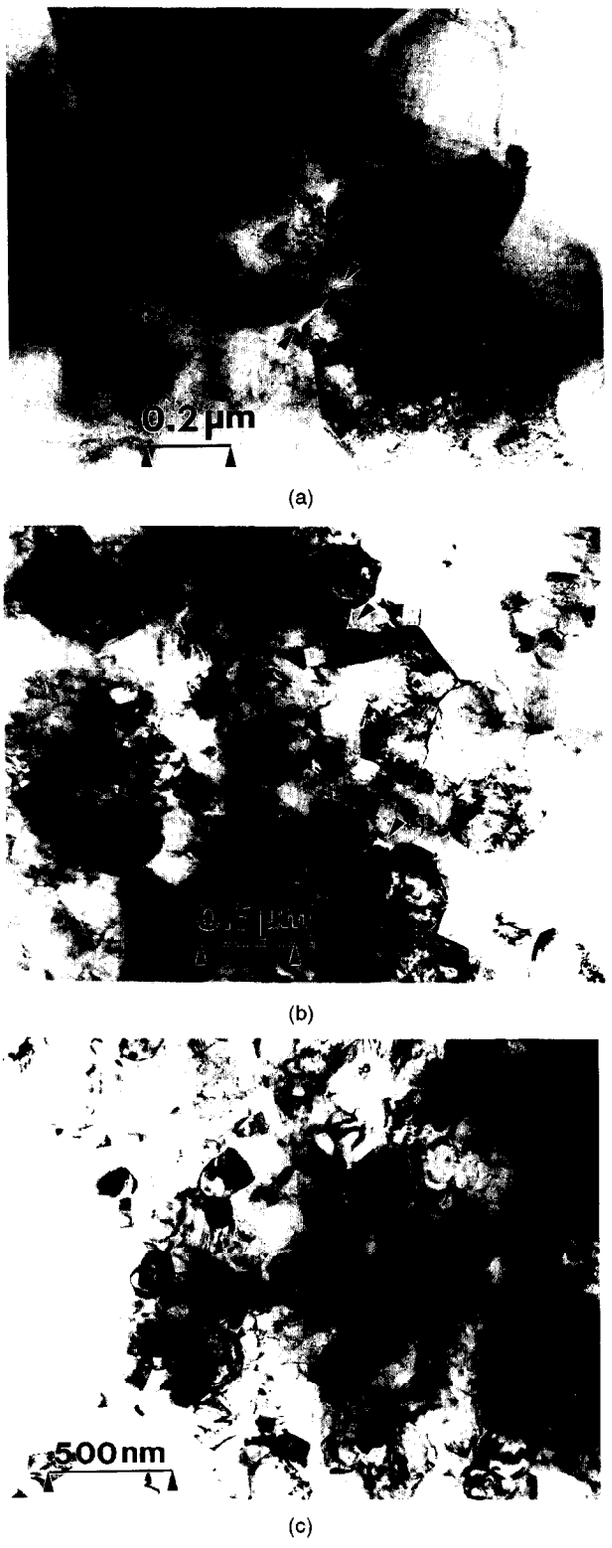

Fig. 1. TEM images showing the microstructure of Y-TZP samples sintered from powder 1 (a), powder 2 (b), and powder 3 (c) respectively. Triple and multiple grain junctions containing larger amounts of amorphous phases are indicated by arrows.

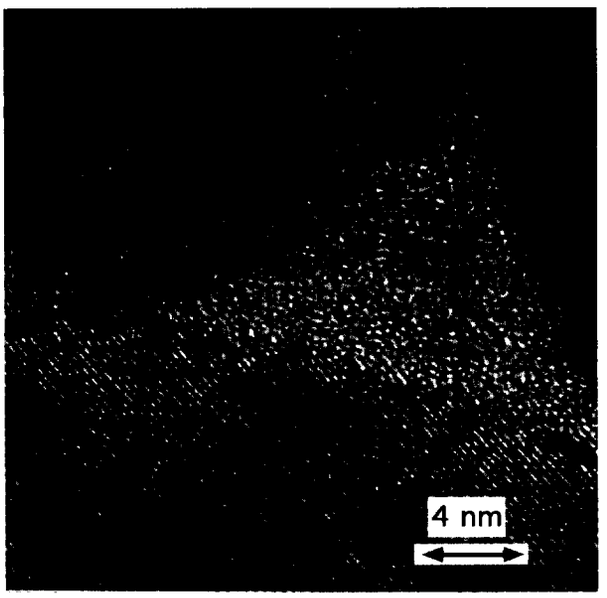

Fig. 2. HRTEM image of a triple pocket in the Y-TZP sintered from powder 1, containing an amorphous phase.

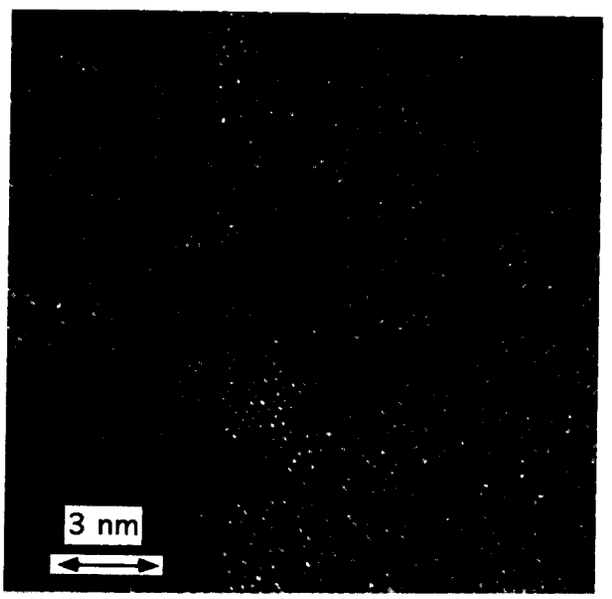

Fig. 3. HRTEM image of a curved large angle tilt grain boundary (both grains are viewed along the same zone axis) in a Y-TZP sintered from powder 1, showing no continuous amorphous film at the grain boundary.

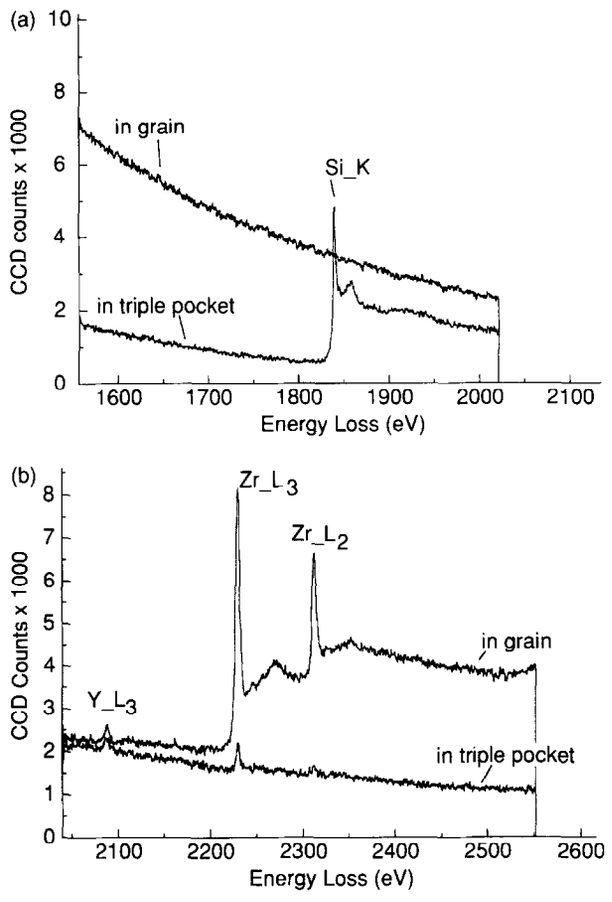

Fig. 4. EEL spectra obtained from the amorphous phase in a triple pocket and from a grain interior in the sample sintered from powder 1. (a) Si K-edge, and (b) Y L-edge and Zr L-edges, showing the presence of Si and Y in the amorphous (silicate) phase, and only a minor amount of Zr.

and (b) shows EEL spectra recorded from the amorphous phase in triple pockets and grain interiors in a sample sintered from powder 1. Figure 4(a) shows the presence of silicon (Si K-edge) in the triple pocket, while no silicon can be detected in the grain. Figure 4(b) shows the Y $L_{2,3}$- and Zr $L_{2,3}$-edges in EEL spectra obtained from a grain interior and from a triple pocket. Yttrium, but much less Zr can be detected in the triple pocket. Al was observed only in a few of the about 10 triple pockets that were analyzed in this study. In the other two samples, sintered from powders 2 and 3, respectively, silicon was detected in the multiple grain junctions only in minor amounts, and in most of the examined triple pockets the content of Si was below the detection limit of the method. The triple pockets contained, however, a significant level of Y and some amount of Zr.

Figure 5(a)–(c) show typical EEL spectra recorded on grain boundaries and in adjacent grains in all three samples. A larger Y signal of the grain boundaries can be observed in all three samples. The Y-content of the grain interiors in the sample sintered from powder 3 was often below the detection limit, although the grain boundaries always showed a large amount of Y. The ratio of Y counts to Zr counts obtained by integration over the respective edges for the samples sintered from powder 1 and 2, respectively, are presented in Fig. 6(a) and (b). As an estimate for the measurement error the scattering of values obtained from the same grain boundary can be used. Silicon was never detected in the grain boundaries of sample sintered from powders 2 and 3, and only occasionally in the sample sintered from powder 1 (starting powder with the highest Si-content).

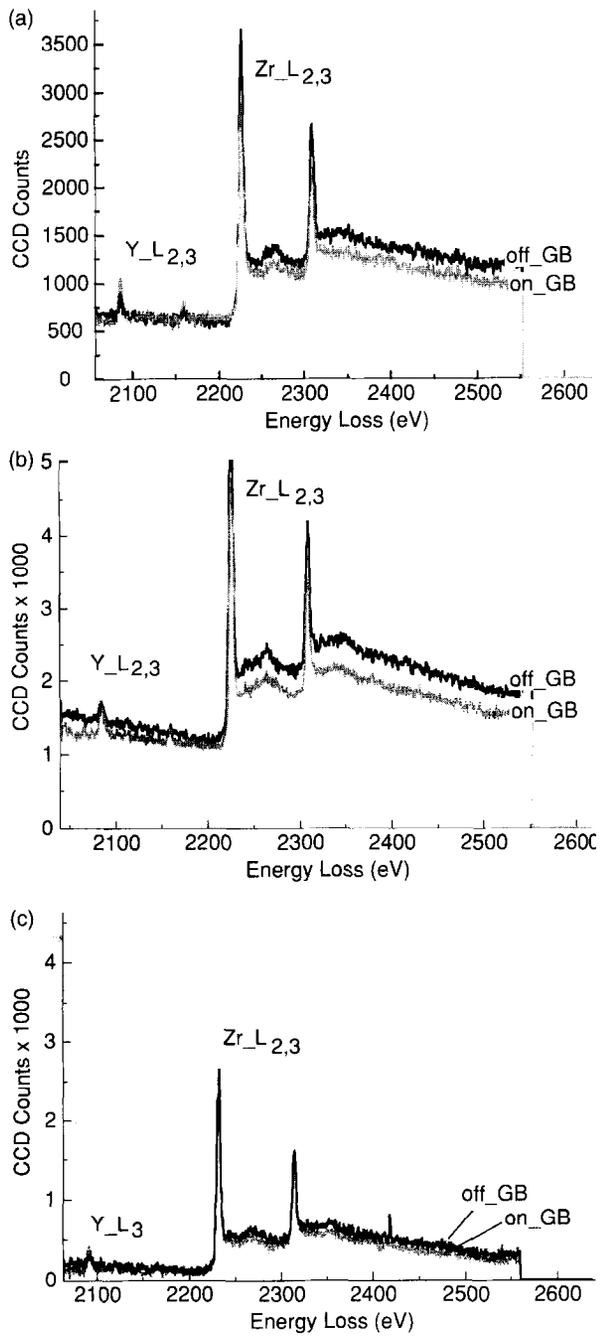

Fig. 5. Y L and Zr L-edges in EEL spectra recorded on grain boundaries ('on-GB'), and one grain next to it ('off-GB'), in the three different ceramics: (a) Y-TZP sintered from powder 1, (b) Y-TZP sintered from powder 2, and (c) from powder 3.

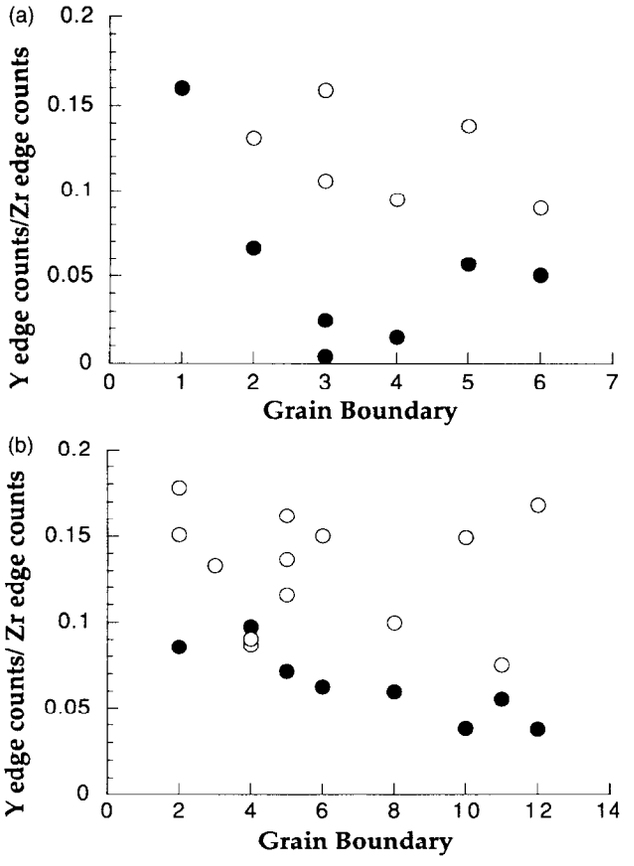

Fig. 6. Y/Zr count ratios obtained by integrating over Y L and Zr L-edges in the Y-TZP sintered from (a) powder 1 and (b) powder 2 respectively, on grain boundaries (open symbols) and in a grain next to it (filled symbols). Where possible, several measurements were performed along one grain boundary.

4 Discussion

Only in the sample sintered from powder 1, which contained the highest amount of silicon, an amorphous silicate phase was present in all triple grain junctions. In this silicate phase, Zr dissolves only in small amounts, whereas Y is a major constituent. However, none of the three samples investigated showed the presence of a continuous amorphous film at the grain boundaries. This result is consistent with those by other authors in high-purity zirconia.[1,16] The observed 'disordering' at the grain boundaries in the sample sintered from powder 1 might be due to the presence of impurities with a grain boundary coverage too thin to form a continuous film, although electron beam radiation damage causing a similar structure cannot be excluded.

Strong Y-segregation to the grain boundaries was observed in all three samples. The absence of a glassy intergranular film indicates that this Y-enrichment is independent from its presence, in contrast to statements by other authors.[8,9] No silicon segregation was observed in the samples sintered from powders 2 and 3, which had the smallest grain size and the lowest Si-content. It is likely that there is not enough silicon present in the sample for a complete coverage of the grain boundary, as observed for similar grain sizes in Ca-stabilized TZP by Aoki *et al.*[1] The latter authors observed a co-segregation of Si and the primary dopant (Ca in their case). Our data, however, suggest that Y strongly segregates even if there is little or no Si present in the samples. Please note that the increased Y/Zr ratio is also due to a lower Zr-content in the grain boundaries, not only due to a higher Y-content. Higher Y/Zr-ratio in the bulk of the grain should also lead to higher Y/Zr ratio in the grain boundary, due to the finite size of the probe, which overlaps into the grain. The scattering of the Y/Zr values obtained from the grain interior is rather small for the sample sintered from powder 2, while it is larger for the values obtained on the grain boundaries. This could be due to a grain size dependence of the grain boundary segregation, and to different deviations of the grain boundary orientation from the edge-on orientation.

The starting powder 3 was fabricated by Y-coating. Therefore, the Y-enrichment of grain boundaries in these samples is likely to be due to this specific fabrication process. This is confirmed by the significantly lower Y-content of the grain interior of the sample sintered from this powder 3. Lawson[17] also measured an inhomogeneous Y-distribution in ceramics obtained from this powder. We assume that the higher fracture toughness values of ceramics prepared from the plasma-coated powders are due to a higher transformability (as confirmed by the presence of the monoclinic phase in the TEM specimens) which is due to a lower Y-content of the grain interior.

5 Conclusions

Enrichment with Y is an inherent property of grain boundaries in fine-grained, high-purity Y-TZP exhibiting grain boundaries free of amorphous films. This segregation will strongly influence important properties of the ceramics, for example the stability of the tetragonal grains, which determines fracture toughness and degradation,[18] or the grain growth in Y-TZP.

Acknowledgements

SS would like to acknowledge support from the European Commission through a TMR grant (contract number FMBICT96-0898). The authors thank Mr. D. Winant for the TEM sample preparation, and Ms. L. Donzel for helpful discussions.

References

1. Aoki, M., Chiang, Y.-M., Kosaki, I., Lee, L. J.-R., Tuller, H. and Liu, Y., Solute segregation and grain-boundary impedance in high-purity stabilized zirconia. *J. Am. Ceram. Soc.*, 1996, **79**, 1169–1180.
2. Hwang, S.-L. and Chen, I.-W., Grain size control of tetragonal zirconia polycrystals using the space charge concept. *J. Am. Ceram. Soc.*, 1990, **73**, 3269–3277.
3. Allemann, L. A., Michel, B., Märki, H.-B., Gauckler, L. J. and Moser, E. M., Grain growth of differently doped zirconia. *J. Europ. Ceram. Soc.*, 1995, **15**, 951–958.
4. Theunissen, G. S. A. M., Winnubst, A. J. A. and Burggraaf, A. J., Surface and grain boundary analysis of doped zirconia ceramics studied by AES and XPS. *J. Mater. Sci.*, 1992, **27**, 5057–5066.
5. Lange, F. F., Controlling grain growth. In. *Ceramic Microstructures '86: Role of Interfaces, Materials Science Research*, **21**, ed. J. A. Pask & A. G. Evans. Plenum Press, New York, 1987, pp. 497–508.
6. Lange, F. F., Transformation-toughened ZrO_2: correlations between grain size control and composition in the system ZrO_2-Y_2O_3. *J. Am. Ceram. Soc.*, 1986, **69**, 240–242.
7. Moser, E. M., Metzger, M. and Gauckler, L. J., SAM/AES analysis of grain boundaries in zirconia ceramics. *Fresenius Anal. Chem*, 1995, **353**, 684–689.
8. Stoto, T., Nauer, M. and Carry, C., Influence of residual impurities on phase partitioning and grain growth processes of Y-TZP materials. *J. Am. Ceram. Soc.*, 1991, **74**, 2615–2621.
9. Boutz, M. M. R., Cheng, C. S., Winnubst, L. and Burggraaf, A. J., Characterization of grain boundaries in superplastically deformed Y-TZP ceramics. *J. Amer. Ceram. Soc.*, 1994, **77**, 2632–2640.
10. Gödickemeier, M., Michel, B., Orliukas, A., Bohac, P., Sasaki, K., Gauckler, L., Heinrich, H., Schwandler, P. and Frei, O., Effect of intergranular films on the electrical conductivity of 3Y-TZP. *J. Mater. Res.*, 1994, **9**, 1228–1240.
11. Gust, M., Goo, G., Wolfenstine, J. and Mecartney, M. L., Influence of amorphous grain boundary phases on the superplastic behavior of 3 mol%-yttria-stabilized tetragonal zirconia polycrystal (3Y-TZP). *J. Am. Ceram. Soc.*, 1993, **76**, 1681–1690.
12. Dransfield, G. P. The use of plasma synthesis and pigment coating technology to produce an yttria-stabilized zirconia having superior properties. In. *Euro-Ceramics*, **1**, ed. G. de Woth, R. A. Tepstrae, R. Metselaar. Elsevier Applied Science, London, 1989, pp. 275–279.
13. Anstis, G. R., Chantikul, P., Lawn, B. R. and Marshall, D. B., A critical evaluation of intendation techniques for measuring fracture toughness: 1, direct crack measurements. *J. Amer. Ceram. Soc.*, 1981, **64**, 533–538.
14. Singh, R., Gill, C., Lawson, S. and Dransfield, G. P., Sintering, microstructure and mechanical properties of commercial Y-TZPs. *J. Mater. Sci.*, 1996, **31**, 6055–6062.
15. Basu, B. and Vleugels, J., unpublished results.
16. Nieh, T. G., Yaney, D. L. and Wadsworth, J., Analysis of grain boundaries in a fine-grained, superplastic, yttria-containing, tetragonal zirconia. *Scr. Metall.*, 1989, **23**, 2007–2011.
17. Lawson, S., The sintering, mechanical and ageing properties of transition metal oxide-doped yttria-tetragonal zirconia polycrystals (Y-TZP), Ph.D. thesis, University of Sunderland, UK, 1993.
18. Schubert, H. and Petzow, G., Microstructural investigations on the stability of yttria-stabilized tetragonal zirconia. In. *Advances in Ceramics*, **24A**: *Science and Technology of Zirconia III*, ed. S. Somiya, N. Yamamoto, and Yanagida, H., The American Ceramic Society, Westerville, 1988, pp. 21–28.